Information Content Carried by Brain Signals Reduces Differentially in MCS and UWS Patients

Shanshan Chen
Beijing Institute of Technology https://orcid.org/0000-0003-2160-0083
Yituo Wang
The 7th Medical Center of Chinese PLA General Hospital
Xiangfeng Meng
The7th Medical Center of PLA General Hospital
Zheng Yang
Beijing Institute of Basic Medical Sciences
Dongdong Weng (crgj@bit.edu.cn)
Beijing Institute of Technology
Xinhuai Wu
The 7th Medical Center of PLA General Hospital
Lubin Wang
Institute of Basic Medical Sciences

Research Article

Keywords: Consciousness, Unresponsive wakefulness syndrome (UWS), Minimally conscious state (MCS), Entropy, Information and integration

Posted Date: May 6th, 2021

DOI: https://doi.org/10.21203/rs.3.rs-338425/v1

Abstract

Objective: Human consciousness is thought to depend on information integration in the brain. How brain injuries affect the information content carried by signals of brain imaging modalities in patients with consciousness disorders has received little attention. Here we propose a novel approach to quantify changes of regional information content in the brain by assessing the entropy delineated by the principal components of regional voxel-based functional imaging signals in clinical MCS and UWS patients.

Method: Resting-state functional imaging was performed in 23 MCS patients, 31 UWS patients, and 20 age-matched healthy individuals.

Results: We show that, as the symptoms of DOC deepen from MCS to UWS, regional information content also was significantly reduced in that order in the sensory and memory systems of the brain. In contrast, with few exceptions, regional information content in high-order cognitive systems remained statistically at a level similar to those in healthy individuals in MCS patients and only showed a significant reduction in UWS patients.

Conclusions and Significance: These findings provide, in the theoretical context of consciousness, novel evidence for a reduction of regional information content as a potential systems-level mechanism of consciousness disorder in MCS and UWS. Further, the findings reveal, for the first time, differential patterns of the reduction of information content in the sensory and memory compared with cognitive systems in MCS and UWS patients, consistent with the manifestations of clinical symptoms in the two DOC patient populations.

Introduction

Understanding the neuropathological mechanisms underlying severe disorders of consciousness (DOC) in patient populations remains one of the central challenges in clinical neuroscience. The information integration theory proposes that the level and richness of consciousness depend on the information capacity and the amount of integrated information in the brain (Oizumi, Albantakis, & Tononi, 2014; Tononi, 2004; Tononi & Koch, 2008). Brain injuries, of either traumatic or anoxic nature, may lead to DOC in patients by reducing the brain's information capacity or disrupting its ability to integrate information (Tononi & Laureys, 2008), as how these two factors may contribute to the suppression of consciousness in general anesthesia (Alkire, Hudetz, & Tononi, 2008). To date, most investigations based on resting-state functional imaging techniques have focused on identifying alterations of functional connectivity in large-scale brain networks in DOC patients as surrogate evidence of disrupted cortical information integration (Boly et al., 2012; Giacino, Fins, Laureys, & Schiff, 2014; Gosseries et al., 2016). In contrast, how brain injuries in DOC patients may alter the information content of brain activity as captured by signals of brain imaging modalities has received little attention. Especially, an understanding of the region-specific alterations of information content across the cortical and subcortical systems of the brain in DOC patients is missing. Filling this gap of knowledge facilitates a deeper understanding of the systems-level

neural mechanisms underlying DOC in patient populations in the theoretical context of human consciousness.

The goal of the study was to determine the changes of regional information content in the resting-state brain activity in two major categories of clinical DOC patients who either are in a minimally conscious state (MCS) or were diagnosed with unresponsive wakefulness syndrome (UWS, previously known as the vegetative state) (Laureys et al., 2010). Brain activity was measured in three groups of study participants, consisting of MCS patients, UWS patients, and age-matched healthy control individuals, using the resting-state functional magnetic resonance imaging (rs-fMRI), which is a unique tool for mapping state-dependent intrinsic, spontaneous brain activities with high spatial precision (Biswal, 2012). The region-specific information content carried by rs-fMRI signals was assessed by the entropy of regional voxel blood-oxygen-level-dependent (BOLD) fMRI signals, based on the definition of entropy in information theory. To make the calculations mathematically tractable, entropy was calculated from the principal components of the voxel BOLD fMRI signals contained within individual anatomical regions. By performing the analysis across neuroanatomically defined brain regions of a standard brain atlas, a quantitative evaluation of the region-specific alterations of information content in the resting-state brain activity can be obtained across the entire brain.

DOC in MCS and UWS were defined with a clear distinction in clinical symptoms between the two conditions, although how to correctly differentiate between patients in the two categories remains one of the most challenging clinical tasks (Giacino et al., 2014; Noirhomme, Brecheisen, Lesenfants, Antonopoulos, & Laureys, 2017). For both conditions, patients exhibit relatively preserved sleep-wake cycles and show reflexive responses to external stimuli. However, MCS patients show minimal, inconsistent, but reproducible behavioral evidence of self or environmental awareness, while UWS patients show no signs of awareness of the self or environment (Giacino & Kalmar, 2005). The differences in the manifestation of clinical symptoms between MCS and UWS suggest that the sensory and cognitive systems of the brain may be differentially affected by brain injuries in the two conditions such that MCS patients may have more preserved functionalities than UWS patients. Insight into this possibility may be gained by determining whether, in comparison with healthy controls, information content carried by signals of rs-fMRI in the sensory and cognitive systems is reduced in a way that scales with the increasing severity of DOC from MCS to UWS.

With the proposed analytical approach, we hypothesized that (1) reduced regional information content is present in both MCS and UWS patient populations relative to healthy individuals, and (2) MCS patients have more preserved regional information content than UWS patients in the sensory and high-order cognitive systems of the brain. As we will show, our results reveal alterations of region-specific information content carried by rs-fMRI signals across the brain in MCS and UWS patients that support our hypotheses. More importantly, the findings show distinct patterns of the reduction of information content in the sensory and memory compared with cognitive systems in MCS and UWS patients that are consistent with the clinical symptoms of DOC in the two conditions.

Materials And Methods

This study was approved by the ethics committee of the Beijing Army General Hospital. Written informed consent was obtained from healthy volunteers and from the legal surrogate of each patient.

Study participants

Study participants included 23 patients in the MCS, 31 patients with UWS, and 20 age-matched healthy control subjects enrolled at Beijing Army General Hospital from 2013 to 2016. At the time of enrollment, the patients had remained in MCS or UWS for at least one month after severe brain injury. Table 1 summarizes the clinical profiles of the patients enrolled in this study. Patients were excluded if they had any of the following clinical conditions: (1) a history of drug or alcohol abuse, (2) a history of psychiatric or neurological illness, or (3) were under sedation or anesthesia during fMRI acquisition.

Imaging data acquisition

Resting-state structural and fMRI data were acquired using a whole-body 3T Signa GE scanner (GE Healthcare, Waukesha, Wisconsin, USA) with a standard transmit-receive head coil. Functional imaging BOLD signals were obtained during a 7-min scan for each subject using the following sequence parameters: repetition time, 2 s; echo time, 25 ms; total volumes, 210; slice thickness, 4.0 mm; in-plane resolution, 3.75 × 3.75 mm; number of slices, 39; flip angle, 90°; field of view, 24.0 cm; matrix size, 64 × 64. High-resolution three-dimensional spoiled gradient-recalled echo axial images were acquired before functional scans with TE/TR/TI, 3.2/8.2/450 ms; slice thickness, 1 mm; 188 slices; flip angle, 7°; field of view, 256 mm; matrix size, 256 × 256.

Imaging data preprocessing

Imaging data preprocessing was conducted using a combination of Analysis of Functional NeuroImages (AFNI, http://afni.nimh.nih.gov/afni), Statistical Parametric Mapping (SPM, http://www.fil.ion.ucl.ac.uk/spm), FMRIB Software Library (FSL, http://www.fmrib.ox.ac.uk), and MATLAB software (MathWorks, Natick, MA, USA). First, T1-weighted anatomical images of each subject were manually transformed into the Talairach space; then, each subject's functional imaging data were registered into the Talairach space with a resampling to a 3 mm cubic voxel size. The first four data points were discarded to reduce the initial transient effects in data acquisition. Subsequent data preprocessing included slice timing correction (*3dTshift* in AFNI), despiking (*3dDespike* in AFNI), and motion correction (*3dvolreg* in AFNI, producing three translational and three rotational parameters for each volume image). Physiological noise was estimated using the average BOLD fMRI signals from regions of white matter and cerebrospinal fluid determined in each individual's anatomical images in the Talairach space. The voxelwise BOLD fMRI signals were then analyzed with a general linear regression model (*3dDeconvolve* in AFNI) using the eight regressors representing noise artifacts from the motion parameters, white matter, and cerebrospinal fluid, respectively. The residual voxelwise time series from the regression analysis were considered as the resting-state BOLD fMRI signals with potential noise contaminations minimized. The denoised functional images were then transformed into the MNI

(Montreal Neuroimaging Institute) space (MNI152; *3dWarp* in AFNI) with a 3-mm cubic voxel size. In the MNI space, functional data were further cleaned by regressing out artifacts originating from the subregions of major vein (e.g., superior sagittal sinus) areas. Next, the cleaned voxelwise BOLD fMRI signals were standardized to z-scores (i.e., zero mean and unity standard deviation) and then bandpass filtered to preserve only the amplitude of low-frequency fluctuations within 0.01–0.1 Hz for the subsequent analysis of regional information content.

Computation of PCA-based entropy of regional voxel BOLD fMRI signals

Regional information content was quantitatively assessed by the entropy (H) of voxel-based BOLD fMRI signals contained within individual neuroanatomical regions,

$$H = (1/2) * \log((2\pi e)^n * \det(COV)), \quad \text{(Eq. 1)}$$

where *n* is the number of voxels (variables), *COV* is the covariance matrix of all voxel BOLD fMRI time series, and *det(COV)* denotes the determinant of the covariance matrix. Eq. 1 assumes that the statistical distribution of the participating signal time series is Gaussian.

When used directly with regional voxel-based BOLD fMRI signals, the entropy formula (Eq. 1) suffers from a practical limitation due to the substantial number of voxels (variables in the signal space) and the strong linear dependency among voxel BOLD time series. This collinearity results in a near-zero determinant of the covariance matrix, making the calculation of entropy using Eq. 1 practically unfeasible. This limitation, however, can be overcome by calculating the entropy of the principal components (PCs) of regional voxel BOLD fMRI signals. Principal component analysis (PCA) is an effective way to convert BOLD fMRI signals into a set of linearly uncorrelated variables (i.e., PCs). The number of the first few significant PCs can be determined by specifying the total percentage of variance explained (PVE), achieving both a reduction of the dimensionality in the signal space and a further reduction of noise with the preprocessed BOLD fMRI signals.

Calculation of the PCA-based entropy of regional voxel BOLD fMRI signals was based on the volumetric rs-fMRI data. The final results were overlaid on the brain surface (*fsaverage* in FreeSurfer) for a better visualization. First, a segmentation of 116 anatomical regions covering the whole brain was obtained using a standard brain atlas (Tzourio-Mazoyer et al., 2002) in the MNI space. For each participant, BOLD fMRI time series of all voxels included in each of the 116 anatomical regions were arranged into a data matrix, resulting in 116 matrices with the column entries of each matrix representing individual voxels (variables) and the row entries representing BOLD signals indexed by time (TR = 2 s). PCA was then conducted with each of the 116 matrices. The number of the first few significant PCs was subsequently determined for each anatomical region by varying the PVE threshold across a range of values, e.g., 70%, 80%, 85%, and 90%, respectively. Next, the covariance matrix of the sets of PCs obtained at each PVE threshold was computed and the corresponding entropy was subsequently obtained (Eq. 1) for each

anatomical region. In our analyses, we found that varying the PVE threshold across a range of values does not significantly alter the results and general conclusions of our study. In this study, we chose to report the primary results obtained at the PVE threshold of 85%.

To show the general trends of changes in entropy (i.e., information content) at the chosen PVE threshold (e.g., 85%) among the MCS, UWS, and healthy control groups, the group mean differences of entropy among the three groups were quantified for each of the 116 anatomical regions. The three paired group comparisons were always arranged in a DOC-deepening order for a better visualization of changes given the same colormap. To quantify changes in entropy in the sensory and high-order cognitive systems of the brain, group paired *t*-tests were conducted in six sets of well-known regions in sensory systems and eight in cognitive systems. The six sets of sensory regions include the (1) sensorimotor cortex, (2) visual cortex, (3) superior temporal gyrus (STG; the auditory cortex), (4) fusiform gyrus (facial information encoding), (5) orbital prefrontal cortex (PFC; reward and olfactory information encoding), and (6) thalamus (relay of sensory information). The eight sets of high-order cognitive regions include the (1) bilateral PFC, (2) medial PFC, (3) insula, (4) anterior cingulate cortex (ACC), (5) middle cingulate cortex (MCC), (6) supramarginal gyrus (SMG) and angular gyrus (AG), (7) inferior and superior parietal lobule (PL), and (8) posterior cingulate cortex (PCC) and precuneus. In addition, group-dependent entropy changes were also examined in two other memory-function-related sets of regions, including the (1) hippocampus and parahippocampal gyrus, and (2) temporal poles. We report the results significant at $P < 0.05$.

Results

Statistical distribution of PC data

We performed a one-sample Kolmogorov-Smirnov test with data from each PC obtained in all 116 anatomical regions and all subjects of the three groups to test the null hypothesis that the data contained in individual PCs comes from a Gaussian distribution at its mean and standard deviation. The results collectively indicted that 99.82%, 99.65%, and 95.05% of all PCs in all healthy control, MCS, and UWS subjects are consistent with the null hypothesis, which was set to be rejected at the 1% significance level. Therefore, an average of more than 98.17% of obtained PCs in healthy individuals and DOC patients can be considered to come from a Gaussian distribution, supporting the calculation of entropy using Eq. 1 based on the covariance matrices of PCs of regional voxel BOLD fMRI signals.

Regional entropy in healthy control, MCS, and UWS subjects

Regional entropy obtained across the entire brain in healthy individuals and patients generally varied in a group-dependent manner, with the highest group mean entropy found in healthy control individuals (Fig. 1A *left*); this was moderately reduced in MCS (Fig. 1A *middle*) and showed a substantial reduction across the entire brain in UWS (Fig. 1A *right*).

A detailed examination of region-specific group mean differences of entropy showed that, relative to healthy individuals, MCS patients showed reduced regional entropy mainly in major sensory regions including the sensorimotor, visual, and auditory cortices; fusiform gyrus; orbital PFC; thalamus; and regions associated with memory functions including the hippocampus, parahippocampal gyrus, and temporal poles (Fig. 1B). In contrast, compared with healthy individuals, UWS patients showed a substantial reduction of group mean entropy across nearly all regions of the brain (Fig. 1C). Of note, the reduction of entropy in several sensory regions (e.g., the sensorimotor and auditory cortices) is especially prominent. It is worth noting that the group mean entropy in the precuneus and PCC showed little difference in UWS patients compared with healthy controls. A comparison of UWS with MCS patients showed a reduction of regional entropy across the entire brain in UWS relative to MCS patients (Fig. 1D), with a more pronounced reduction in multiple areas of the temporal lobe and bilateral PFC.

Group-dependent changes in entropy in sensory, memory, and cognitive systems

Based on observations of regional group mean entropy in the three groups, a further analysis of group-dependent changes in entropy in the eight sets of brain regions of the two DOC categories was performed. Brain regions in one category are related to sensory and memory functions, including the sensorimotor, visual, and auditory cortices; fusiform gyrus; orbital PFC; thalamus; hippocampus and parahippocampal gyrus; and temporal poles. Brain regions in the other category are related to high-order cognitive functions, including the bilateral PFC, medial PFC, insula, ACC, MCC, SMG and AG, inferior and superior PL, and PCC and precuneus.

Compared with healthy individuals, regional entropy in the sensory and memory systems is significantly reduced in the same order as the symptoms of DOC deepen from MCS to UWS (Fig. 2A). That is, MCS patients showed a significant reduction of entropy relative to healthy control individuals and UWS patients relative to MCS patients. Among the sensory regions examined, we found only one exception to the trend of changes in the visual cortex, in which no statistical difference was found between healthy control individuals and MCS patients. In comparison, regional entropy in high-order cognitive systems remained at a level statistically similar to that in healthy individuals and in MCS patients and only showed a significant reduction in UWS patients (Fig. 2B). Among the examined sets of cognitive regions, an exception to the trend of changes occurred with the PCC and precuneus, in which no group-dependent differences in the amount of entropy were found.

Discussion

Differences in the systems-level neuropathological mechanisms that underlie the clinical symptoms of DOC between patients in the MCS and with UWS remain incompletely understood (Giacino et al., 2014). Using a novel PCA-based approach to quantitatively assess the entropy carried by rs-fMRI signals in individual neuroanatomically defined brain regions (Tzourio-Mazoyer et al., 2002), we show that, relative to healthy control individuals, the MCS is associated with a reduction of information content, as quantified by entropy of regional BOLD rs-fMRI signals, primarily in the sensory and memory but not high-

order cognitive systems. In contrast, UWS is associated with a reduction of information content in all sensory, memory, and cognitive systems relative to healthy control individuals and MCS patients. The significance of the findings can be better appreciated in the contexts of the differences in clinical symptoms between the MCS and UWS as well as the theories of human consciousness.

Theoretical studies of human consciousness and investigations of the neuropathological mechanisms underlying DOC in clinical patients mutually inform each other. According to the information integration theory (Oizumi et al., 2014; Tononi, 2004; Tononi & Koch, 2008), the level and richness of consciousness are related to the information capacity and the amount of integrated information in the brain. Brain injuries in DOC patients may lead to a diminished state of consciousness by reducing the information capacity or disrupting information integration in the brain. During the past decade, extensive rs-fMRI-based studies have examined disruptions of the integrity of functional connections in large-scale brain networks in DOC patients (Boly et al., 2012; Giacino et al., 2014). Altered and mostly reduced function connectivities have been evidenced in the default mode network (Boly et al., 2009; Guldenmund, Vanhaudenhuyse, Boly, Laureys, & Soddu, 2012; Soddu et al., 2012; Soddu et al., 2011; Vanhaudenhuyse et al., 2010), thalamocortical networks (Crone et al., 2014; Laureys et al., 2000; Zhou et al., 2011), and multiple intrinsic connectivity networks (Crone et al., 2014; Demertzi et al., 2015; Demertzi et al., 2014; Heine et al., 2012; Long et al., 2016) in coma, MCS, and UWS patients. The altered functional connections in these large-scale networks were often taken as surrogate evidence of disrupted/reduced cortical information integration that may underlie DOC in patient populations. In contrast, to our knowledge, no other studies have directly addressed, especially in a region-specific manner, the possible alterations of information capacity in the brain as reflected by the signals of brain imaging modalities in DOC patients based on plausible computational measures. An element of the novelty of the present study stems from its theory-driven analytical approach that allows the obtained results to be directly discussed and interpreted in the context of the current theories of consciousness (Oizumi et al., 2014; Tononi, 2004; Tononi & Koch, 2008).

The incessant changes of spontaneous configurations of intrinsic brain activity in resting wakefulness in healthy individuals are considered to underlie the ongoing stream of consciousness that encompasses spontaneous mentation, imagery, task-independent thoughts, daydreaming, etc. (Mason et al., 2007). Such intrinsic brain activities can be captured by or reflected in signals of brain imaging modalities. It is plausible to assume that the richness or repertoire of the configurations of intrinsic brain activities as measured by rs-fMRI may be altered in various cortical and subcortical systems of the brain in DOC patients. From an information theory perspective, the amount of information generated by a dynamic system is equivalent to the degree of uncertainty of its intrinsic states measured by the system's entropy, assuming that the noise influence is minimized (Ben-Naim, 2012). A high entropy of intrinsic brain activity indicates a high degree of uncertainty and, therefore, a rich repertoire of intrinsic metastable states that the brain can access over time (Carhart-Harris et al., 2014; Haldeman & Beggs, 2005; Shanahan, 2010; Tognoli & Kelso, 2014). Though entropy can be assessed at different spatial scales of functional imaging measurement, e.g., from a single voxel to large-scale network level, the current study focuses on examining entropy at the spatial scale defined by individual neuroanatomical regions

(Tzourio-Mazoyer et al., 2002). Macroscopic anatomical boundaries have a general, though imperfect, relation to functional boundaries. By performing such region-based analysis, insights may be gained with respect to how the amount of entropy or information content as carried by rs-fMRI signals may be altered in various sensory, memory, and high-order cognitive systems in MCS and UWS patients compared with healthy control individuals. Thus, our findings provide, within the current theoretical context of human consciousness, direct evidence that diminished consciousness in MCS and UWS is associated with a reduction of information content in the brain as carried by regional BOLD rs-fMRI signals.

It is worth emphasizing that, computationally, a direct calculation of entropy (Eq. 1) using the regional voxel BOLD fMRI signals is not feasible because of the presence of a high degree of collinearity among individual voxel signal time series within the same anatomical region. In this work, we proposed a novel PCA-based approach to quantify entropy carried by regional BOLD fMRI signals, circumventing this computational limitation. Moreover, we found that data in a predominant portion (> 98.17%) of obtained PCs conforms to a Gaussian distribution, supporting the use of Eq. 1 for the entropy calculation. We consider that the observed predominant Gaussian distribution is mainly due to fact that data in each PC is a linear combination of all voxel BOLD fMRI signals in individual neuroanatomical regions. According to the central limit theorem, the resulting PC time series converges to a Gaussian distribution.

An important finding of the present study is the differential patterns of the reduction of information content in the sensory and memory compared with cognitive systems in MCS and UWS patients relative to healthy control individuals. Specifically, information content is only reduced in the sensory and memory but not in high-order cognitive systems in MCS patients; in contrast, a significant reduction of information content occurred in all sensory, memory, and cognitive systems in UWS patients compared with both healthy control individuals and MCS patients. Such differential reductions of information content in sensory and memory compared with cognitive systems in MCS and UWS patients are consistent with the manifestations of clinical symptoms in the two DOC patient populations. First, MCS patients show inconsistent but reproducible signs of awareness of the self and environment, which requires that the high-order cognitive systems still be functional to a reasonable extent for the possibility of generating meaningful perceptions. In parallel, MCS patients recently were found to have brain activation patterns to transcranial magnetic stimulation that are as widespread and differentiated as observed in healthy individuals and locked-in patients (Gosseries et al., 2015). On the other hand, the very limited capability of showing an evident possession of awareness in MCS patients is plausibly related to a functional degradation in the sensory and memory systems of the brain, as reflected by a reduction of entropy/information content in these regions. Second, for UWS patients who show no signs of any awareness at all, it is plausible that the ability in UWS patients to form any meaningful perception in the high-order cognitive systems is seriously compromised, together with a much severer degradation of functions in sensory and memory systems, even compared with MCS patients. Indeed, a convincing piece of evidence supporting our conclusions is that as the symptoms of DOC deepen from MCS to UWS patients relative to healthy control individuals, the reduction of regional information content also becomes significantly enlarged in all the sensory, memory, and cognitive systems of the brain in UWS compared with MCS patients. Such a trend of changes is less likely occasional but more convincingly a

reflection of the differences in the severity of the clinical symptoms of DOC between MCS and UWS patients.

With respect to the exception to the trend of changes in the sensory systems, i.e., the visual cortex (Fig. 2A, last bar group), we consider that the variations in maintaining eye-opening and eye-closing conditions in healthy individuals and especially in MCS patients during scan may have played a role. However, it is however puzzling to us that the exception in the cognitive systems, the PCC and precuneus, an area that has been particularly implicated in consciousness and DOC in terms of its metabolism and functional connectivity (Boly et al., 2012; Giacino et al., 2014; Hannawi, Lindquist, Caffo, Sair, & Stevens, 2015), did not show significant differences in entropy among the three groups (Fig. 2B, last bar group). We speculate that the observation may be related to the inherent anatomical heterogeneity in the PCC and precuneus (Leech & Sharp, 2014), which may confine significant changes of entropy in rs-fMRI signals. Clearly, it should be highlighted that the regional information content measured by entropy, metabolism, task-related activation, and functional connectivity are not the same and that they reflect different functional properties of mass neural activities of the brain.

A few limitations of the present study are noted. First, entropy was derived from rs-fMRI BOLD signals that are indirect, coarse-grained indicators of neuronal activity. Thus, interpretations of the results shall be in the context of imaging signal acquisition. Second, estimating entropy requires noise influence to be minimized. Our concern about the denoising issue, however, was mitigated because of the observation that the trend of reduction in information content scales with severity of DOC in MCS and UWS patients, which was unlikely led by noise. In addition, PCA performed in this study eliminated a portion of nuisance components, offering an additional procedure for signal denoising. Third, another possibility is that systematic changes in the physiological conditions (blood pressure, breathing and heart beat rates, etc.) across subjects in the three groups may produce artificial changes in BOLD fMRI signals (e.g., the amplitude and variance) that affect the analysis of entropy. Considering this possibility, we performed a voxelwise standardization of BOLD fMRI signals (normalizing to zero mean and unity standard deviation, i.e., z-score) before applying low-pass filtering. Therefore, the effects of alterations of physiological parameters on the obtained results should be minimal.

In summary, using a novel PCA-based approach to quantitatively assess the entropy carried by rs-fMRI signals across individual neuroanatomically defined brain regions, we show in the theoretical context that the diminished state of consciousness in MCS and UWS patients is associated with a reduction in information content in the brain compared with healthy individuals. Importantly, our findings reveal differential patterns of reduction in information content in the sensory and memory compared with cognitive systems in MCS and UWS patients, which are consistent with their respective clinical symptoms. Together, the findings suggest a systems-level mechanism in terms of the alteration of regional information content in the brain that may underlie consciousness disorders in MCS and UWS patients.

Abbreviations

ACC = anterior cingulate cortex, AG = angular gyrus, BOLD = blood-oxygen-level-dependent, CRS-R = coma recovery scale-revised, DOC = disorders of consciousness, MCS = minimally conscious state, MCC = middle cingulate cortex motor area, PC = principal component, PCA = principal component analysis, PCC = posterior cingulate cortex, PFC = prefrontal cortex, rs-fMRI = resting-state functional magnetic resonance imaging, PL = parietal lobule, PVE = percentage of variance explained, SMG = supramarginal gyrus, UWS = unresponsive wakefulness syndrome.

Declarations

Funding: This work is partially supported by the National Natural Science Foundation of China (No.61902026).

Conflict of Interest: The authors declare no conflict of interest.

Ethical approval: All procedures performed in studies involving human participants were in accordance with the ethical standards of the institutional and/or national research committee and with the 1964 Helsinki declaration and its later amendments or comparable ethical standards.

Consent to participate: Written informed consent was obtained from healthy volunteers and from the legal surrogate of each patient.

Consent for publication: The content included in the submission has not been published and it is not under consideration for publication elsewhere.

Code availability: Not applicable.

References

1. Alkire, M. T., Hudetz, A. G., & Tononi, G. (2008). Consciousness and anesthesia. *Science, 322*(5903), 876–880. doi:10.1126/science.1149213.
2. Ben-Naim, A. (2012). *Entropy and the second law: interpretation and misss-interpretationsss*. New Jersey; London: World Scientific.
3. Biswal, B. B. (2012). Resting state fMRI: a personal history. *Neuroimage, 62*(2), 938–944. doi:10.1016/j.neuroimage.2012.01.090.
4. Boly, M., Massimini, M., Garrido, M. I., Gosseries, O., Noirhomme, Q., Laureys, S., & Soddu, A. (2012). Brain connectivity in disorders of consciousness. *Brain Connect, 2*(1), 1–10. doi:10.1089/brain.2011.0049.
5. Boly, M., Tshibanda, L., Vanhaudenhuyse, A., Noirhomme, Q., Schnakers, C., Ledoux, D.,.. . Laureys, S. (2009). Functional connectivity in the default network during resting state is preserved in a vegetative but not in a brain dead patient. *Hum Brain Mapp, 30*(8), 2393–2400. doi:10.1002/hbm.20672.

6. Carhart-Harris, R. L., Leech, R., Hellyer, P. J., Shanahan, M., Feilding, A., Tagliazucchi, E.,.. . Nutt, D. (2014). The entropic brain: a theory of conscious states informed by neuroimaging research with psychedelic drugs. *Front Hum Neurosci, 8*, 20. doi:10.3389/fnhum.2014.00020.
7. Crone, J. S., Soddu, A., Holler, Y., Vanhaudenhuyse, A., Schurz, M., Bergmann, J.,.. . Kronbichler, M. (2014). Altered network properties of the fronto-parietal network and the thalamus in impaired consciousness. *Neuroimage Clin, 4*, 240–248. doi:10.1016/j.nicl.2013.12.005.
8. Demertzi, A., Antonopoulos, G., Heine, L., Voss, H. U., Crone, J. S., de Los Angeles, C.,.. . Laureys, S. (2015). Intrinsic functional connectivity differentiates minimally conscious from unresponsive patients. *Brain, 138*(Pt 9), 2619–2631. doi:10.1093/brain/awv169.
9. Demertzi, A., Gomez, F., Crone, J. S., Vanhaudenhuyse, A., Tshibanda, L., Noirhomme, Q.,.. . Soddu, A. (2014). Multiple fMRI system-level baseline connectivity is disrupted in patients with consciousness alterations. *Cortex; a journal devoted to the study of the nervous system and behavior, 52*, 35–46. doi:10.1016/j.cortex.2013.11.005.
10. Giacino, J. T., Fins, J. J., Laureys, S., & Schiff, N. D. (2014). Disorders of consciousness after acquired brain injury: the state of the science. *Nat Rev Neurol, 10*(2), 99–114. doi:10.1038/nrneurol.2013.279.
11. Giacino, J. T., & Kalmar, K. (2005). Diagnostic and prognostic guidelines for the vegetative and minimally conscious states. *Neuropsychol Rehabil, 15*(3–4), 166–174. doi:10.1080/09602010443000498.
12. Gosseries, O., Pistoia, F., Charland-Verville, V., Carolei, A., Sacco, S., & Laureys, S. (2016). The Role of Neuroimaging Techniques in Establishing Diagnosis, Prognosis and Therapy in Disorders of Consciousness. *Open Neuroimag J, 10*, 52–68. doi:10.2174/1874440001610010052.
13. Gosseries, O., Sarasso, S., Casarotto, S., Boly, M., Schnakers, C., Napolitani, M.,.. . Rosanova, M. (2015). On the cerebral origin of EEG responses to TMS: insights from severe cortical lesions. *Brain Stimul, 8*(1), 142–149. doi:10.1016/j.brs.2014.10.008.
14. Guldenmund, P., Vanhaudenhuyse, A., Boly, M., Laureys, S., & Soddu, A. (2012). A default mode of brain function in altered states of consciousness. *Arch Ital Biol, 150*(2–3), 107–121. doi:10.4449/aib.v150i2.1373.
15. Haldeman, C., & Beggs, J. M. (2005). Critical branching captures activity in living neural networks and maximizes the number of metastable States. *Phys Rev Lett, 94*(5), 058101. doi:10.1103/PhysRevLett.94.058101.
16. Hannawi, Y., Lindquist, M. A., Caffo, B. S., Sair, H. I., & Stevens, R. D. (2015). Resting brain activity in disorders of consciousness: a systematic review and meta-analysis. *Neurology, 84*(12), 1272–1280. doi:10.1212/WNL.0000000000001404.
17. Heine, L., Soddu, A., Gomez, F., Vanhaudenhuyse, A., Tshibanda, L., Thonnard, M.,.. . Demertzi, A. (2012). Resting state networks and consciousness: alterations of multiple resting state network connectivity in physiological, pharmacological, and pathological consciousness States. *Front Psychol, 3*, 295. doi:10.3389/fpsyg.2012.00295.

18. Laureys, S., Celesia, G. G., Cohadon, F., Lavrijsen, J., Leon-Carrion, J., & Sannita, W. G... . European Task Force on Disorders of, C. (2010). Unresponsive wakefulness syndrome: a new name for the vegetative state or apallic syndrome. *BMC Med*, *8*, 68. doi:10.1186/1741-7015-8-68.
19. Laureys, S., Faymonville, M. E., Luxen, A., Lamy, M., Franck, G., & Maquet, P. (2000). Restoration of thalamocortical connectivity after recovery from persistent vegetative state. *Lancet, 355*(9217), 1790–1791. doi:S0140673600022716 [pii].
20. Leech, R., & Sharp, D. J. (2014). The role of the posterior cingulate cortex in cognition and disease. *Brain, 137*(Pt 1), 12–32. doi:10.1093/brain/awt162.
21. Long, J. Y., Xie, Q. Y., Ma, Q., Urbin, M. A., Liu, L. Q., Weng, L.,.. . Huang, R. W. (2016). Distinct Interactions between Fronto-Parietal and Default Mode Networks in Impaired Consciousness. *Scientific Reports, 6*. doi:ARTN 3886610.1038/srep38866.
22. Mason, M. F., Norton, M. I., Van Horn, J. D., Wegner, D. M., Grafton, S. T., & Macrae, C. N. (2007). Wandering minds: the default network and stimulus-independent thought. *Science, 315*(5810), 393–395. doi:10.1126/science.1131295.
23. Noirhomme, Q., Brecheisen, R., Lesenfants, D., Antonopoulos, G., & Laureys, S. (2017). "Look at my classifier's result": Disentangling unresponsive from (minimally) conscious patients. *Neuroimage, 145*(Pt B), 288–303. doi:10.1016/j.neuroimage.2015.12.006.
24. Oizumi, M., Albantakis, L., & Tononi, G. (2014). From the phenomenology to the mechanisms of consciousness: Integrated Information Theory 3.0. *PLoS Comput Biol, 10*(5), e1003588. doi:10.1371/journal.pcbi.1003588.
25. Shanahan, M. (2010). Metastable chimera states in community-structured oscillator networks. *Chaos (Woodbury, N.Y.), 20*(1), 013108. doi:10.1063/1.3305451.
26. Soddu, A., Vanhaudenhuyse, A., Bahri, M. A., Bruno, M. A., Boly, M., Demertzi, A.,.. . Noirhomme, Q. (2012). Identifying the default-mode component in spatial IC analyses of patients with disorders of consciousness. *Hum Brain Mapp, 33*(4), 778–796. doi:10.1002/hbm.21249.
27. Soddu, A., Vanhaudenhuyse, A., Demertzi, A., Bruno, M. A., Tshibanda, L., Di, H.,.. . Noirhomme, Q. (2011). Resting state activity in patients with disorders of consciousness. *Funct Neurol, 26*(1), 37–43. doi:4838 [pii].
28. Tognoli, E., & Kelso, J. A. (2014). The metastable brain. *Neuron, 81*(1), 35–48. doi:10.1016/j.neuron.2013.12.022.
29. Tononi, G. (2004). An information integration theory of consciousness. *BMC Neurosci, 5*, 42. doi:10.1186/1471-2202-5-42.
30. Tononi, G., & Koch, C. (2008). The neural correlates of consciousness: an update. *Ann N Y Acad Sci, 1124*, 239–261. doi:10.1196/annals.1440.004.
31. Tononi, G., & Laureys, S. (2008). The neurology of consciousness: An overview. In S. Laureys & G. Tononi (Eds.), *The Neurology of Consciousness: Cognitive Neuroscience and Neuropathology*: Elsevier Ltd.

32. Tzourio-Mazoyer, N., Landeau, B., Papathanassiou, D., Crivello, F., Etard, O., Delcroix, N.,.. . Joliot, M. (2002). Automated anatomical labeling of activations in SPM using a macroscopic anatomical parcellation of the MNI MRI single-subject brain. *Neuroimage, 15*(1), 273–289. doi:10.1006/nimg.2001.0978.
33. Vanhaudenhuyse, A., Noirhomme, Q., Tshibanda, L. J., Bruno, M. A., Boveroux, P., Schnakers, C.,.. . Boly, M. (2010). Default network connectivity reflects the level of consciousness in non-communicative brain-damaged patients. *Brain, 133*(Pt 1), 161–171. doi:10.1093/brain/awp313.
34. Zhou, J., Liu, X., Song, W., Yang, Y., Zhao, Z., Ling, F.,.. . Li, S. J. (2011). Specific and nonspecific thalamocortical functional connectivity in normal and vegetative states. *Conscious Cogn, 20*(2), 257–268. doi:10.1016/j.concog.2010.08.003.

Tables

Table1. Demographic and clinical characteristics of patients

Patient ID	Gender	Age	Months since onset	Etiology	Lesion information	CRS-R score	Diagnosis
1	M	23	5	TBI	Right basal ganglia lesion	7	MCS
2	F	28	1	TBI	Brainstem atrophy	15	MCS
3	F	31	3	TBI	Left thalamus and brainstem atrophy	11	MCS
4	M	60	7	TBI	Diffuse white matter damage	11	MCS
5	M	58	12	TBI	Bilateral frontal contusion and brainstem hemorrhage	8	MCS
6	M	29	9	TBI	Multi-focal contusion	18	MCS
7	M	41	1	TBI	DAI and subcortical atrophy	11	MCS
8	F	27	10	TBI	Multi-focal contusion and left frontoparietal hemorrhage	12	MCS
9	M	39	1	HI	Left basal ganglia hemorrhage and brain atrophy	17	MCS
10	M	23	3	HI	Brainstem atrophy	10	MCS
11	F	28	9	Poisoning	Anoxia caused by drug poisoning	10	MCS
12	M	61	2	HI	Left basal ganglia and left thalamus hemorrhage	11	MCS
13	M	42	3	HI	Brain atrophy	7	MCS
14	M	42	2	HI	Left thalamus hemorrhage	8	MCS
15	M	53	7	HI	Right basal ganglia hemorrhage	11	MCS
16	M	45	9	HI	Brainstem hemorrhage	9	MCS
17	M	32	6	HI	Multi-focal hemorrhagic lesion	11	MCS
18	M	28	2	CPA	n/a	9	MCS
19	M	28	5	CA	n/a	8	MCS

20	M	46	2	CPA	n/a	9	MCS
21	M	51	6	CA	n/a	9	MCS
22	M	45	3	HIE	n/a	10	MCS
23	M	36	5	TBI	n/a	10	MCS
24	F	46	15	TBI	n/a	7	VS
25	F	58	2	TBI	Left parietal-occipital lesion and brainstem hemorrhage	3	VS
26	F	66	1	TBI	Bilateral frontoparietal lesion	6	VS
27	M	34	3	TBI	DAI and brain atrophy	6	VS
28	M	46	2	HIE	Brainstem hemorrhage	6	VS
29	M	52	4	HIE	Brainstem hemorrhage	5	VS
30	M	39	3	HIE	Left basal ganglia hemorrhage	7	VS
31	F	53	3	HIE	Brainstem hemorrhage	5	VS
32	M	49	10	HI	Brainstem lesion	7	VS
33	M	58	6	HI	Right temporal lobe hemorrhage	7	VS
34	F	60	4	HIE	Anoxia caused by anesthesia	6	VS
35	M	42	6	HI	Right hemisphere and brainstem lesions	7	VS
36	F	28	5	HIE	n/a	6	VS
37	M	40	4	HI	Brainstem hemorrhage	4	VS
38	F	29	28	Eclampsia	Intraparenchymal hemorrhage and severe brain atrophy	7	VS
39	F	42	1	CA	Anoxia caused by amniotic fluid embolism	7	VS
40	M	43	2	CA	Cardiac arrest caused by coronary heart diseases	5	VS
41	F	51	6	CPA	n/a	6	VS
42	M	51	3	CPA	n/a	7	VS
43	F	35	2	CPA	Bilateral frontoparietal	7	VS

					lesions		
44	M	41	2	CPA	Multi-focal cerebral infarction	5	VS
45	F	71	30	CPA	Multi-focal cerebral infarction and brain atrophy	7	VS
46	F	50	6	CPA	n/a	5	VS
47	M	45	9	HIE	n/a	5	VS
48	F	73	2	HIE	n/a	7	VS
49	M	62	2	HIE	n/a	3	VS
50	M	30	2	HIE	n/a	6	VS
51	M	18	8	Asphyxia	n/a	6	VS
52	M	26	54	HIE	n/a	6	VS
53	F	n/a	2	CPA	n/a	n/a	VS
54	M	71	6	TBI	Right tempo-parietal lesion and DAI	3	VS

TBI: traumatic brain injury; HI: Hemorrhagic cerebral infarction; HIE: hypoxic-ischemic encephalopathy; CA: cardiac arrest; CPA: cardiopulmonary arrest; DAI: diffused axonal injury; F: female; M: male

Figures

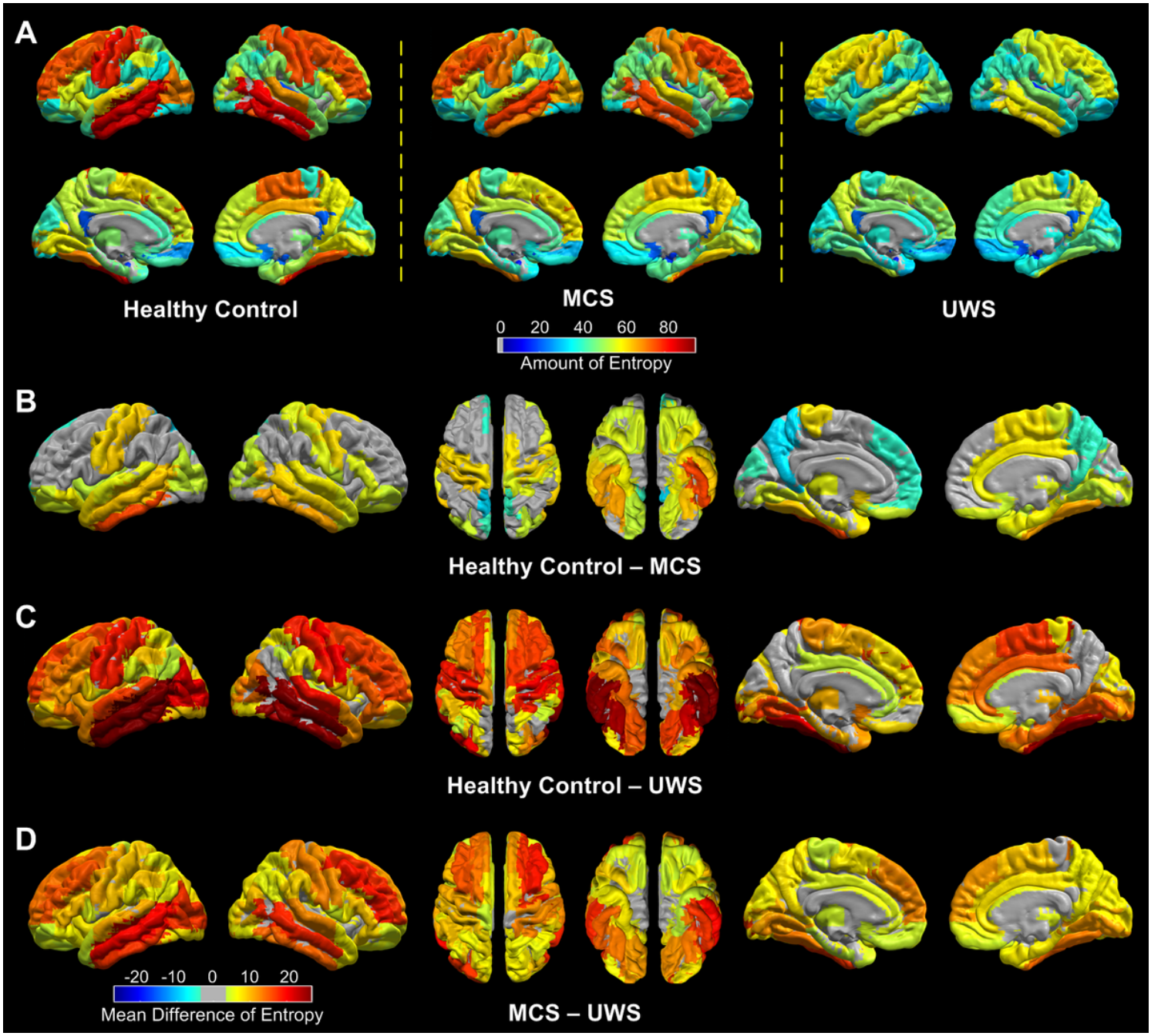

Figure 1

(A) The amount of region-specific entropy obtained at the PVE threshold of 85% in healthy control, MCS, and UWS subjects. Note a decreasing trend of entropy from healthy control to MCS and to UWS subjects. (B) Group mean differences in entropy between healthy control and MCS subjects. Regions with differences near zero are depicted in gray to allow emphasis of changes in other regions. (C) Group mean differences in entropy between healthy control and UWS subjects. (C) Group mean differences in entropy between MCS and UWS subjects.

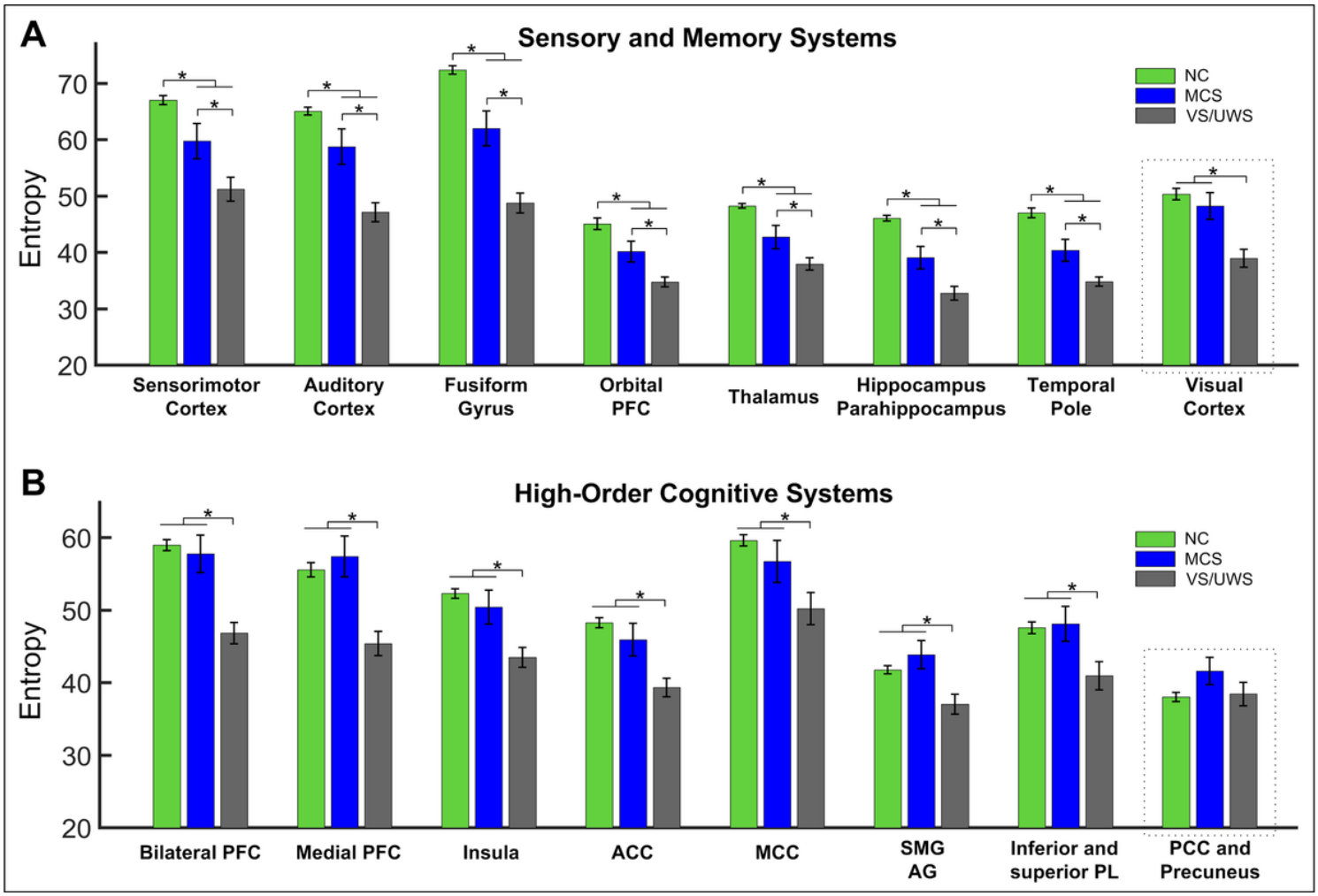

Figure 2

Group-dependent changes of entropy in the sensory and memory compared with high-order cognitive systems. (A) Changes of regional entropy in the eight sets of brain regions involved in sensory and memory functions. (B) Changes of regional entropy in the eight sets regions involved in high-order cognitive functions. In both (A) and (B), the exceptions with respect to the trends of changes in each panel, i.e., the visual cortex in (A) and the PCC and precuneus in (B), are highlighted by boxes with dashed lines. (*: P <= 0.05, error bars represent the standard error of measurement.)